

Maximization of fundamental frequencies of axially compressed laminated truncated conical shells against fiber orientation



Hsuan-Teh Hu*, Pei-Jen Chen

Department of Civil Engineering, National Cheng Kung University, Tainan 701, Taiwan, ROC

ARTICLE INFO

Article history:

Received 24 April 2015

Received in revised form

2 September 2015

Accepted 7 September 2015

Keywords:

Maximization

Fundamental frequency

Laminated truncated conical shell

Axially compressive force

ABSTRACT

Free vibration analyses of laminated truncated conical shells subjected to axial compressive forces are carried out by employing the Abaqus finite element program. The fundamental frequencies of these truncated conical shells with a given material system are then maximized with respect to fiber orientations by using the golden section method. Through parametric studies, the influences of the end condition, shell length, shell radius ratio and the compressive force on the maximum fundamental frequencies, the associated optimal fiber orientations and the associated vibration modes are demonstrated and discussed.

© 2015 Elsevier Ltd. All rights reserved.

1. Introduction

Due to light weight and high strength, the use of fiber reinforced composite laminated materials in the aerospace industry has increased rapidly in recent years. The truncated conical shell configuration is widely used in aircraft, spacecraft, rocket and missile, which are frequently subjected to dynamic loads in service. Hence, knowledge of dynamic characteristics of truncated conical shells constructed of fiber-reinforced laminated materials, such as their fundamental frequencies, is essential [1].

The fundamental frequencies of laminated truncated conical shells highly depend on ply orientations, boundary conditions, and geometric variables such as shell radius ratio and shell length [1–12]. In addition, the fundamental frequencies of laminated structures are significantly influenced by the initial stresses within them [13–19]. Therefore, for laminated truncated conical shells with a given material system, geometric shape, initial stress and boundary condition, the proper selection of appropriate lamination to maximize the fundamental frequency of the shells becomes an interesting problem [20–22].

There are many computational methods available today for the vibration analysis of laminated conical shells, such as finite

element method (FEM) [9], discrete singular convolution (DSC) [23,24], generalized differential quadrature (GDQ) [25] and meshless method [26]. Comparisons of the superiority and effectiveness of these methods are not the scope and the focus of this paper. Since the FEM can easily simulate the complicated and irregular geometries of structures, it is selected in this investigation to calculate the nature frequencies of the laminated truncated conical shells.

Research on the subject of structural optimization has been reported by many investigators [27]. Among various optimization schemes, the method of golden section method [28,29] is very efficient and has been successfully applied to many engineering problems. In this investigation, optimization of fiber-reinforced laminated truncated conical shells to maximize their fundamental frequencies with respect to fiber orientations is performed by using the golden section method. The fundamental frequencies of laminated truncated conical shells are calculated by using the Abaqus finite element program [30]. In the paper, the constitutive equations for fiber-composite laminate, vibration analysis and golden section method are briefly reviewed. Then the influences of the end condition, shell length, shell radius ratio and the compressive force on the maximum fundamental frequencies, the associated optimal fiber orientations and the associated vibration modes of laminated truncated conical shells are presented. Finally, important conclusions obtained from this study are given.

* Corresponding author. Fax: +886 6 2358542.

E-mail address: hthu@mail.ncku.edu.tw (H.-T. Hu).

2. Constitutive matrix for fiber-composite laminae

In the finite element analysis, the laminated truncated conical

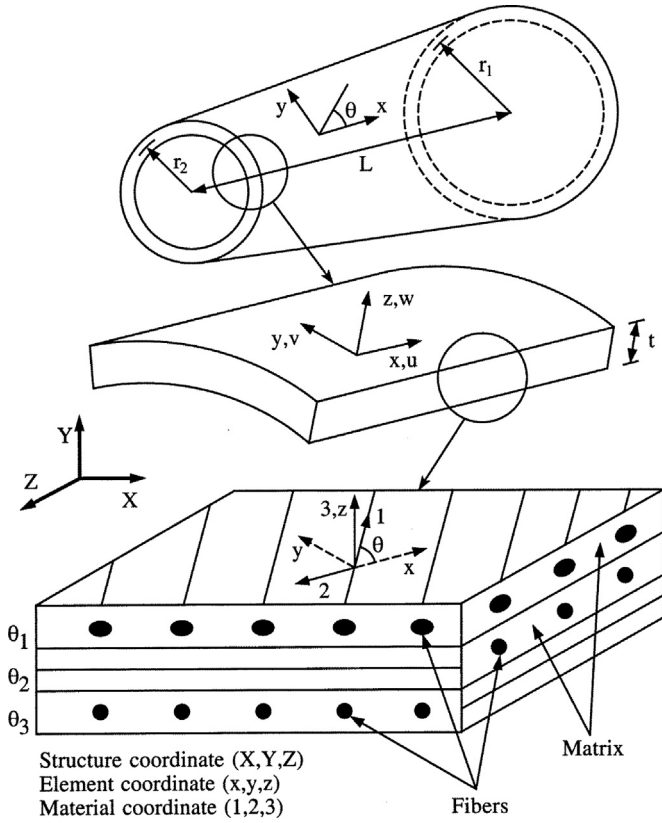


Fig. 1. Material, element and structure coordinates of laminated truncated conical shells.

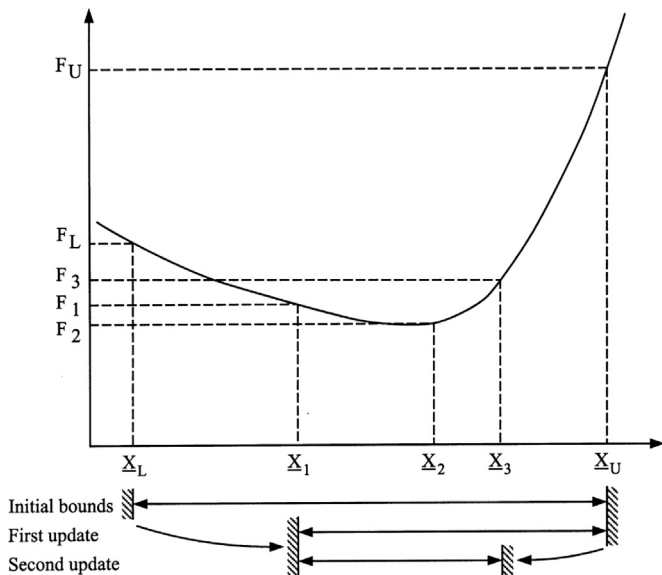


Fig. 2. The golden section method.

shells are modeled by eight-node isoparametric shell elements with six degrees of freedom per node (three displacements and three rotations). The reduced integration rule together with hourglass stiffness control is employed to formulate the element stiffness matrix [30].

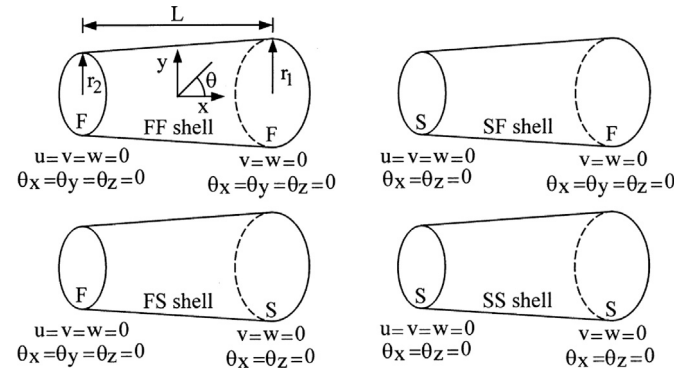


Fig. 3. Truncated conical shells with various end conditions.

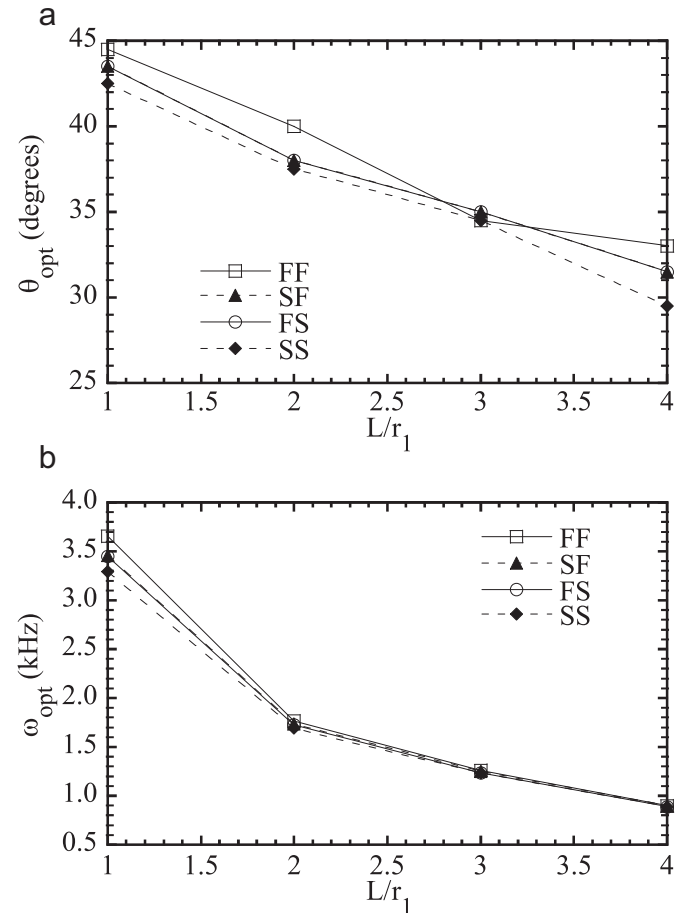


Fig. 4. Effect of end condition and L/r_1 ratio on optimal fiber angle and optimal fundamental frequency of $[\pm \theta/90_2/0]_2$ laminated truncated conical shells with axial compressive force ($r_1 = 10$ cm, $r_2 = 10$ cm, $N/N_{cr} = 0.2$).

During the analysis, the constitutive matrices of composite materials at element integration points must be calculated before the stiffness matrices are assembled from element level to global level. For fiber-composite laminate materials, each lamina can be considered as an orthotropic layer. The stress–strain relations for a lamina in the material coordinate (1,2,3) (Fig. 1) at an element integration point can be written as

$$\{\sigma'\} = [Q_1]\{\epsilon'\}, \quad \{\tau'\} = [Q_2]\{\gamma'\} \quad (1)$$

$$[Q_1] = \begin{bmatrix} \frac{E_{11}}{1 - \nu_{12}\nu_{21}} & \frac{\nu_{12}E_{22}}{1 - \nu_{12}\nu_{21}} & 0 \\ \frac{\nu_{21}E_{11}}{1 - \nu_{12}\nu_{21}} & \frac{E_{22}}{1 - \nu_{12}\nu_{21}} & 0 \\ 0 & 0 & G_{12} \end{bmatrix} \quad [Q_2] = \begin{bmatrix} \alpha_1 G_{13} & 0 \\ 0 & \alpha_2 G_{23} \end{bmatrix} \quad (2)$$

where $\{\sigma'\} = \{\sigma_1, \sigma_2, \tau_{12}\}^T$, $\{\tau'\} = \{\tau_{13}, \tau_{23}\}^T$, $\{\epsilon'\} = \{\epsilon_1, \epsilon_2, \gamma_{12}\}^T$, $\{\gamma'\} = \{\gamma_{13}, \gamma_{23}\}^T$. The α_1 and α_2 in Eq. (2) are shear correction factors, which are calculated in Abaqus by assuming that the transverse shear energy through the thickness of laminate is equal to that in unidirectional bending [30,31].

The constitutive equations for the lamina in the element coordinate (x,y,z) then become

$$\{\sigma\} = [Q_1]\{\epsilon\}, \quad [Q_1] = [T_1]^T [Q_1'] [T_1] \quad (3)$$

$$\{\tau\} = [Q_2]\{\gamma\}, \quad [Q_2] = [T_2]^T [Q_2'] [T_2] \quad (4)$$

$$[T_1] = \begin{bmatrix} \cos^2 \theta & \sin^2 \theta & \sin \theta \cos \theta \\ \sin^2 \theta & \cos^2 \theta & -\sin \theta \cos \theta \\ -2 \sin \theta \cos \theta & 2 \sin \theta \cos \theta & \cos^2 \theta - \sin^2 \theta \end{bmatrix}, \quad [T_2] = \begin{bmatrix} \cos \theta & \sin \theta \\ -\sin \theta & \cos \theta \end{bmatrix} \quad (5)$$

where $\{\sigma\} = \{\sigma_x, \sigma_y, \tau_{xy}\}^T$, $\{\tau\} = \{\tau_{xz}, \tau_{yz}\}^T$, $\{\epsilon\} = \{\epsilon_x, \epsilon_y, \gamma_{xy}\}^T$, $\{\gamma\} = \{\gamma_{xz}, \gamma_{yz}\}^T$ and θ is measured counterclockwise about the z axis from the element local x-axis to the material 1-axis. The element coordinate system (x,y,z) is a curvilinear local system (Fig. 1) that is different from the structural global coordinate (X,Y,Z). While the element x axis is in the longitudinal direction of the truncated conical shell, element y and z axes are in the circumferential and the radial directions of the truncated conical shell. Let $\{\epsilon_0\} = \{\epsilon_{x0}, \epsilon_{y0}, \gamma_{xy0}\}^T$ be the in-plane strains at the mid-

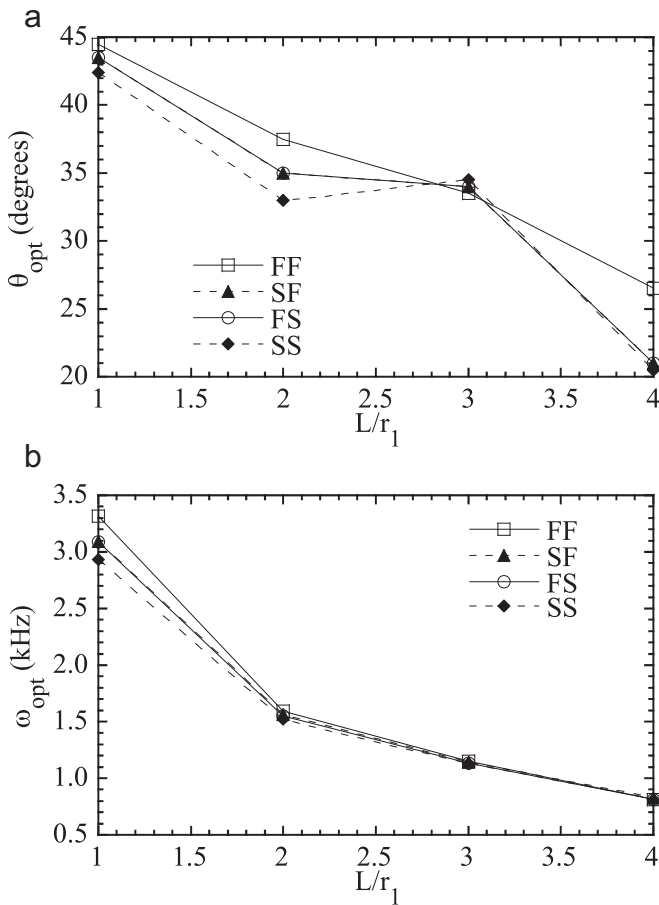


Fig. 5. Effect of end condition and L/r_1 ratio on optimal fiber angle and optimal fundamental frequency of $[\pm \theta/90_2/0]_{2s}$ laminated truncated conical shells with axial compressive force ($r_1 = 10$ cm, $r_2 = 10$ cm, $N/N_{cr} = 0.4$).

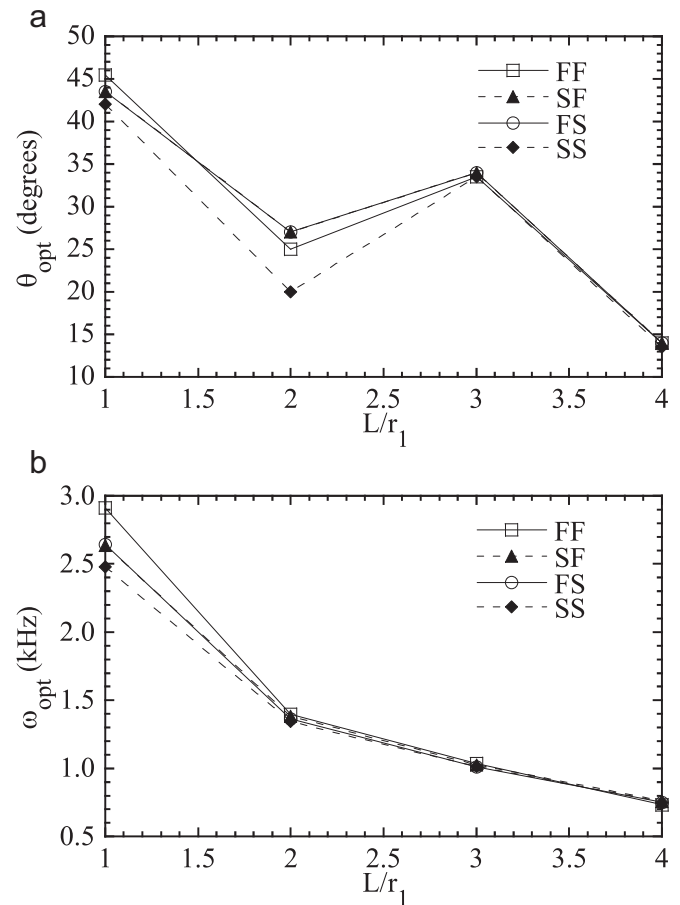


Fig. 6. Effect of end condition and L/r_1 ratio on optimal fiber angle and optimal fundamental frequency of $[\pm \theta/90_2/0]_{2s}$ laminated truncated conical shells with axial compressive force ($r_1 = 10$ cm, $r_2 = 10$ cm, $N/N_{cr} = 0.6$).

surface of the laminate section, $\{\kappa\} = \{\kappa_x, \kappa_y, \kappa_{xy}\}^T$ the curvatures, and h the total thickness of the section. If there are n layers in the layup, the stress resultants, $\{N\} = \{N_x, N_y, N_{xy}\}^T$, $\{M\} = \{M_x, M_y, M_{xy}\}^T$ and $\{V\} = \{V_x, V_y\}^T$, can be defined as

$$\begin{Bmatrix} \{N\} \\ \{M\} \\ \{V\} \end{Bmatrix} = \int_{-h/2}^{h/2} \begin{Bmatrix} \{\sigma\} \\ z\{\sigma\} \\ \{\tau\} \end{Bmatrix} dz = \sum_{j=1}^n \begin{bmatrix} (z_{jt} - z_{jb})Q_{11} & \frac{1}{2}(z_{jt}^2 - z_{jb}^2)Q_{11} & [0] \\ \frac{1}{2}(z_{jt}^2 - z_{jb}^2)Q_{11} & \frac{1}{3}(z_{jt}^3 - z_{jb}^3)Q_{11} & [0] \\ [0]^T & [0]^T & (z_{jt} - z_{jb})Q_{22} \end{bmatrix} \begin{Bmatrix} \{\epsilon_0\} \\ \{\kappa\} \\ \{\tau\} \end{Bmatrix} \quad (6)$$

where z_{jt} and z_{jb} are the distance from the mid-surface of the section to the top and the bottom of the j -th layer respectively. The $[0]$ is a 3 by 2 matrix with all the coefficients equal to zero.

3. Vibration analysis

For the free vibration analysis of an undamped structure, the equation of motion of the structure can be written in the following form [32]:

$$[M]\{\ddot{D}\} + [K]\{D\} = \{0\} \quad (7)$$

where $\{D\}$ is a vector for the unrestrained nodal degrees of freedoms, $\{\ddot{D}\}$ an acceleration vector, $[M]$ the mass matrix of the structure, $[K]$ the stiffness matrix of the structure, and $\{0\}$ a zero vector. Since $\{D\}$ undergoes harmonic motion, we can express

$$\{D\} = \{\bar{D}\} \sin \omega t; \quad \{\ddot{D}\} = -\omega^2 \{\bar{D}\} \sin \omega t \quad (8)$$

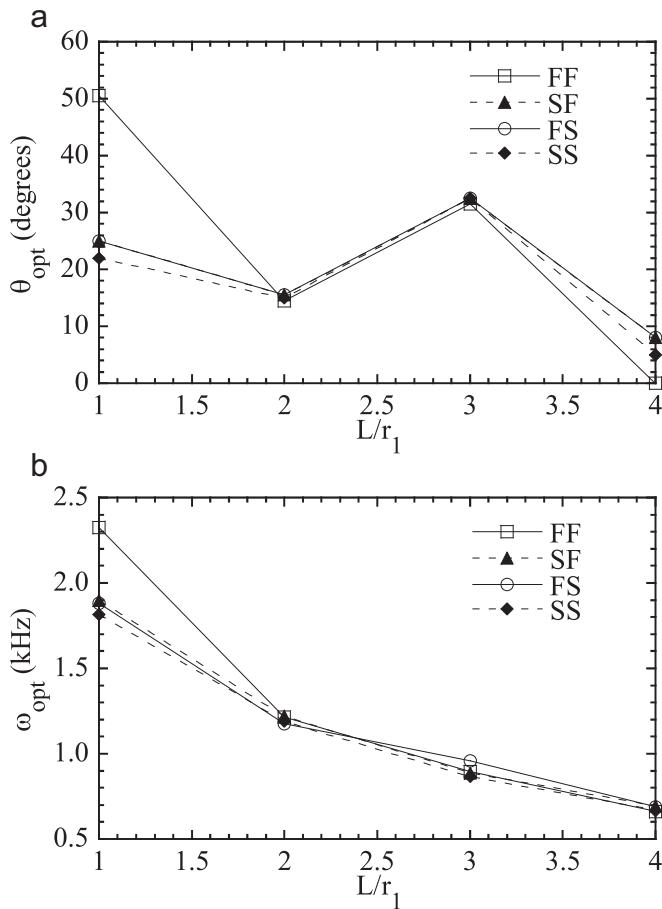


Fig. 7. Effect of end condition and L/r_1 ratio on optimal fiber angle and optimal fundamental frequency of $[\pm \theta/90_2/0]_{2s}$ laminated truncated conical shells with axial compressive force ($r_1 = 10$ cm, $r_2 = 10$ cm, $N/N_{cr} = 0.8$).

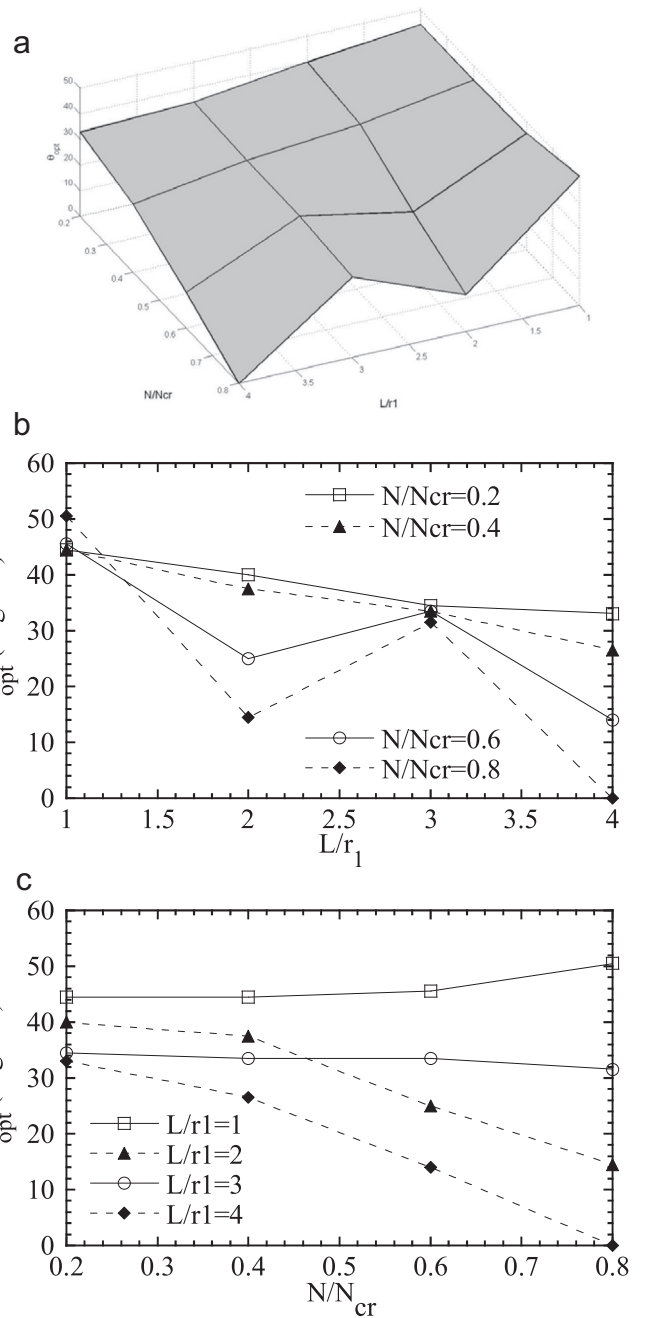


Fig. 8. Effect of L/r_1 ratio and N/N_{cr} ratio on optimal fiber angle of $[\pm \theta/90_2/0]_{2s}$ laminated truncated conical shells with two fixed ends ($r_1 = 10$ cm, $r_2 = 10$ cm).

where $\{\bar{D}\}$ vector contains the amplitudes of $\{D\}$ vector. Then Eq. (7) can be written in an eigenvalue expression as

$$([K] - \omega^2[M])\{\bar{D}\} = \{0\} \tag{9}$$

When a laminated truncated conical shell is subjected to compressive force, initial stresses are generated in the panel. Consequently, the stiffness matrix $[K]$ in Eq. (9) can be separated

into two matrices as

$$[K] = [K_L] + [K_\sigma] \tag{10}$$

The $[K_L]$ is the traditional linear stiffness matrix and $[K_\sigma]$ is a geometric stress stiffness matrix due to the initial stresses. Then Eq. (9) becomes

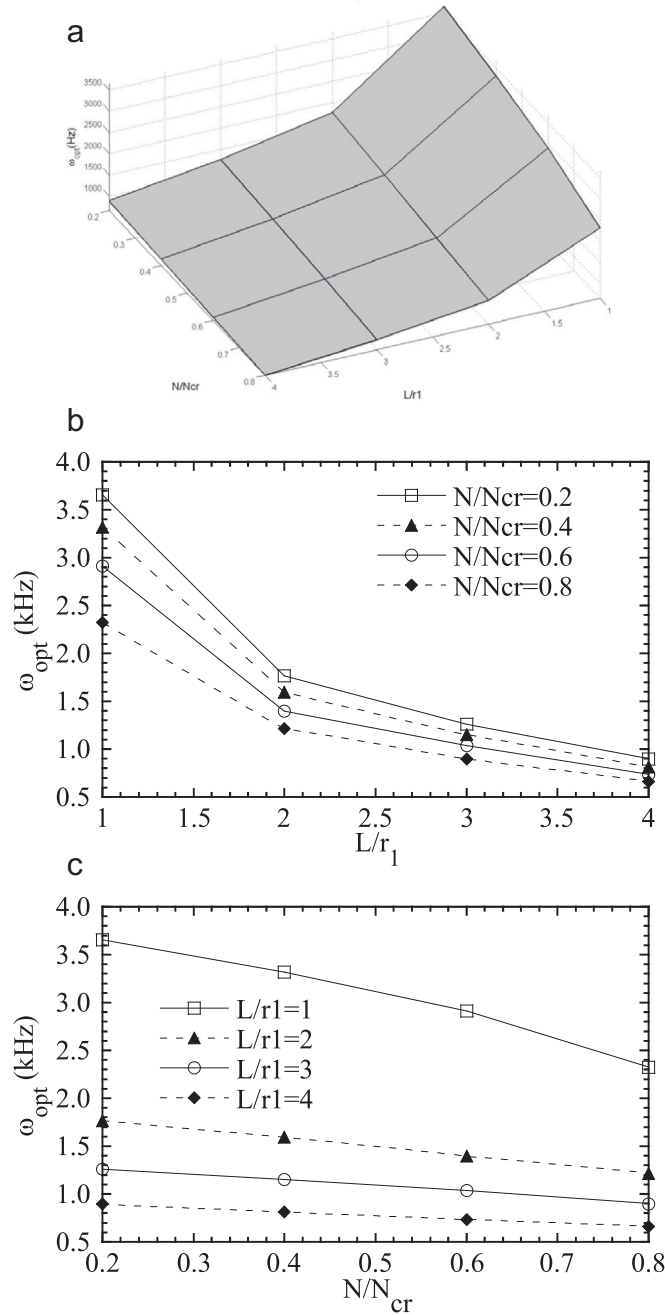


Fig. 9. Effect of L/r_1 ratio and N/N_{cr} ratio on optimal fundamental frequency of $[\pm \theta/90_2/0]_2$ laminated truncated conical shells with two fixed ends ($r_1 = 10$ cm, $r_2 = 10$ cm).

$$([K_L] + [K_\sigma] - \omega^2[M])\{\bar{D}\} = \{0\} \tag{11}$$

The preceding equation is an eigenvalue expression. If $\{\bar{D}\}$ is not a zero vector, we must have

$$|[K_L] + [K_\sigma] - \omega^2[M]| = 0 \tag{12}$$

In Abaqus, a subspace iteration procedure [30] is used to solve for the natural frequencies ω , and the eigenvectors (or vibration modes) $\{\bar{D}\}$. The obtained smallest natural frequency (fundamental frequency) is then the objective function for maximization.

4. Golden section method

We begin by presenting the golden section method [28,29] for determining the minimum of the unimodal function F , which is a function of the independent variable X . It is assumed that lower bound X_L and upper bound X_U on X are known and the minimum

can be bracketed (Fig. 2). In addition, we assume that the function has been evaluated at both bounds and the corresponding values are F_L and F_U . Now we can pick up two intermediate points X_1 and X_2 such that $X_1 < X_2$ and evaluate the function at these two points to provide F_1 and F_2 . Because F_1 is greater than F_2 , now X_1 forms a new lower bound and we have a new set of bounds, X_1 and X_U . We can now select an additional point, X_3 , for which we evaluate F_3 . It is clear that F_3 is greater than F_2 , so X_3 replaces X_U as the new upper bound. Repeating this process, we can narrow the bounds to whatever tolerance is desired.

To determine the method for choosing the interior points X_1, X_2, X_3, \dots , we pick the values of X_1 and X_2 to be symmetric about the center of the interval and satisfying the following expressions:

$$X_U - X_2 = X_1 - X_L \tag{13}$$

$$\frac{X_1 - X_L}{X_U - X_L} = \frac{X_2 - X_1}{X_U - X_1} \tag{14}$$

Let τ be a number between 0 and 1. We can define the interior

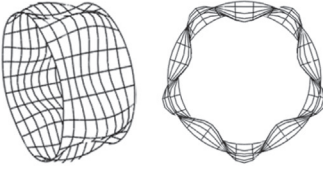
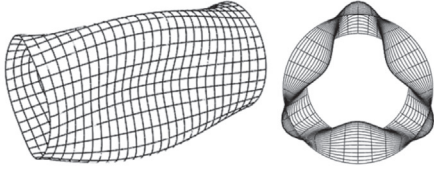
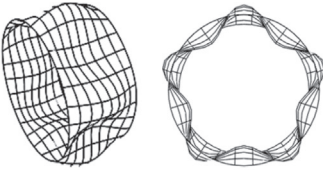
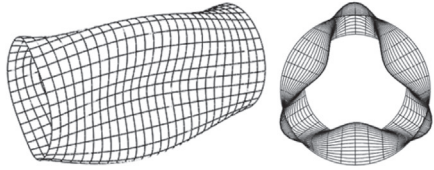
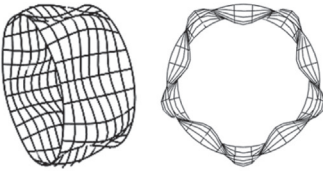
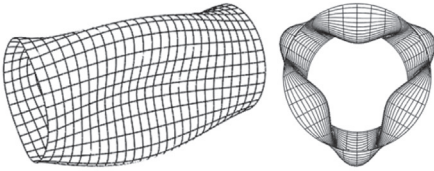
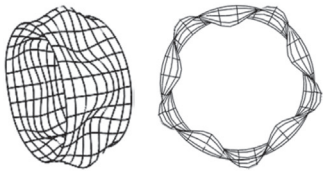
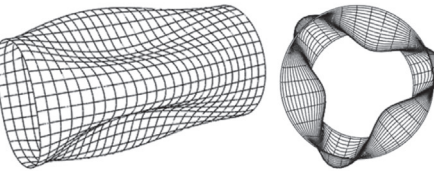
N/N_{cr}	$L/r_1 = 1$	$L/r_1 = 4$
0.2	 <p>$\omega_{opt} = 3.655 \text{ Hz}$</p>	 <p>$\omega_{opt} = 0.894 \text{ Hz}$</p>
0.4	 <p>$\omega_{opt} = 3.316 \text{ Hz}$</p>	 <p>$\omega_{opt} = 0.812 \text{ Hz}$</p>
0.6	 <p>$\omega_{opt} = 2.911 \text{ Hz}$</p>	 <p>$\omega_{opt} = 0.733 \text{ Hz}$</p>
0.8	 <p>$\omega_{opt} = 2.324 \text{ Hz}$</p>	 <p>$\omega_{opt} = 0.661 \text{ Hz}$</p>

Fig. 10. Fundamental vibration modes of $[\pm \theta/90_2/0]_{2s}$ laminated truncated conical shells with two fixed ends and under optimal fiber angles ($r_1 = 10 \text{ cm}$, $r_2 = 10 \text{ cm}$).

points \underline{X}_1 and \underline{X}_2 to be

$$\underline{X}_1 = (1 - \tau)\underline{X}_L + \tau\underline{X}_U \tag{15a}$$

$$\underline{X}_2 = \tau\underline{X}_L + (1 - \tau)\underline{X}_U \tag{15b}$$

Substituting Eqs. (15a) and (15b) into Eq. (14), we obtain

$$\tau^2 - 3\tau + 1 = 0 \tag{16}$$

Solving the above equation, we obtain $\tau = 0.38197$. The ratio $(1 - \tau)/\tau = 1.61803$ is the famous “golden section” number. For a problem involving the estimation of the maximum of a one-variable function F , we need only minimize the negative of the function, that is, minimize $-F$.

5. Numerical analysis

The accuracy of the eight-node shell element in Abaqus program for frequency analysis has been verified by the authors

[17,18] and good agreements are obtained between the numerical results and the analytical solution or experimental data. Hence, it is confirmed that the accuracy of the shell element in Abaqus program is good enough to analyze the vibration behavior of laminated structures.

5.1. Laminated truncated conical shells with shell radius ratio $r_2/r_1 = 1$ and with various boundary conditions, lengths and axial compressive forces

In this section, laminated truncated conical shells with four types of boundary conditions (Fig. 3) are considered, which are two ends fixed (denoted by FF), left end simply supported and right end fixed (denoted by SF), left end fixed and right end simply supported (denoted by FS), and two ends simply supported (denoted by SS). The axial compressive force N is applied to the right end of the shell along the longitudinal x direction of the shell. The radius of the conical shell at the right end, r_1 , is equal to 10 cm and the radius of the shell at the left end, r_2 , is also equal to 10 cm

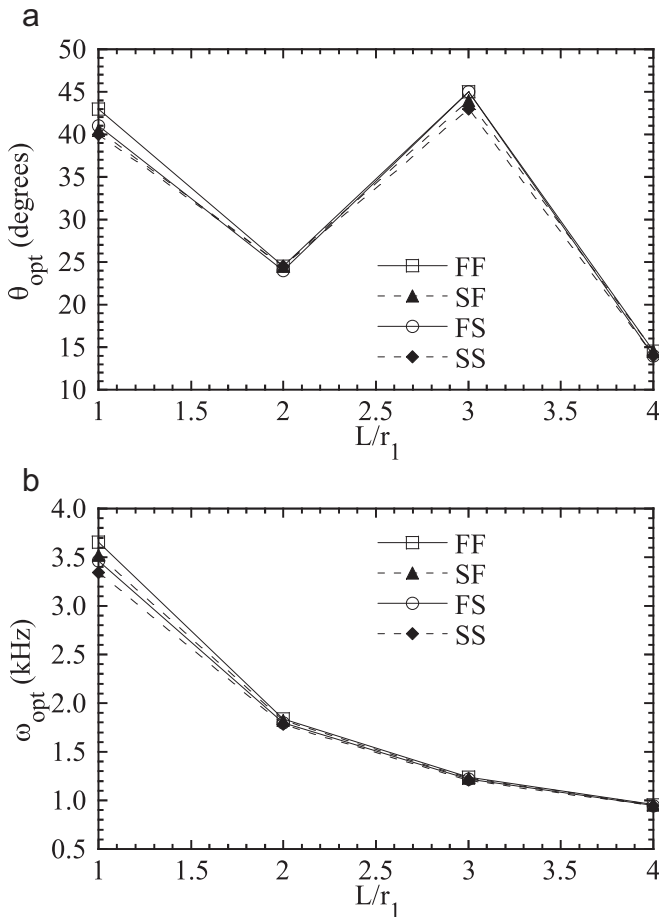


Fig. 11. Effect of end condition and L/r_1 ratio on optimal fiber angle and optimal fundamental frequency of $[\pm \theta/90_2/0]_{2s}$ laminated truncated conical shells with axial compressive force ($r_1 = 10$ cm, $r_2 = 8$ cm, $N/N_{cr} = 0.2$).

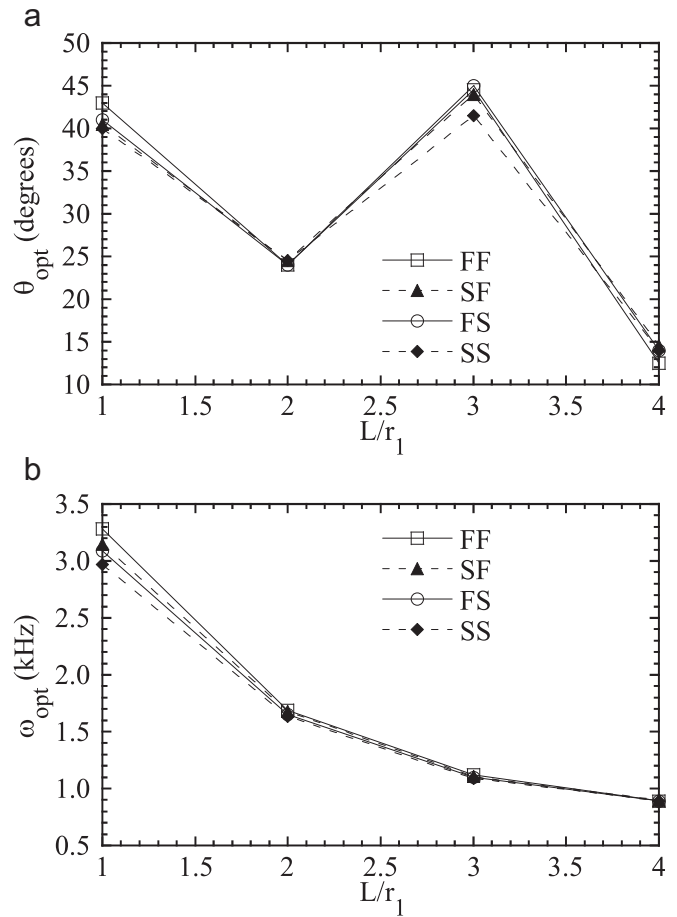


Fig. 12. Effect of end condition and L/r_1 ratio on optimal fiber angle and optimal fundamental frequency of $[\pm \theta/90_2/0]_{2s}$ laminated truncated conical shells with axial compressive force ($r_1 = 10$ cm, $r_2 = 8$ cm, $N/N_{cr} = 0.4$).

(radius ratio $r_2/r_1 = 1$). The length of the shell L varies between 10 cm and 40 cm. The laminate layup of the conical shell is $[\pm \theta/90_2/0]_{2s}$ and the thickness of each ply is 0.125 mm. To study the influence of axial compressive force N on the results of optimization, $N = 0.2N_{cr}$, $0.4N_{cr}$, $0.6N_{cr}$, and $0.8N_{cr}$, are selected for analysis, where N_{cr} is the linearized critical buckling load of the laminated truncated conical shell. The lamina consists of Graphite/Epoxy and material constitutive properties are taken from the data of Crawley [33], which are $E_{11} = 128$ GPa, $E_{22} = 11$ GPa, $G_{23} = 1.53$ GPa, $G_{12} = G_{13} = 4.48$ GPa, $\nu_{12} = 0.25$, and $\rho = 1500$ kg/m³. The convergent analyses of the finite element mesh have been performed by the authors [9]. No symmetry simplifications are made for those laminated truncated conical shells.

To find the optimal fiber angle θ_{opt} and the associated optimal fundamental frequency ω_{opt} , we can express the optimization problem as:

$$\text{Maximize: } \omega(\theta) \tag{17a}$$

$$\text{Subjected to: } 0^\circ \leq \theta \leq 90^\circ \tag{17b}$$

Before the golden section method is carried out, the fundamental frequency ω of the laminated truncated conical shell is calculated by employing the Abaqus finite element program for every 10° increment in θ angle to locate the maximum point approximately. Then proper upper and lower bounds are selected so that the fundamental frequency is a unimodal function within the search region. Finally, the golden section method is carried out to find the maximum. The optimization process is terminated when an absolute tolerance (the difference of the two intermediate points between the upper bound and the lower bound) $\Delta\theta \leq 0.5^\circ$ is reached.

Fig. 4 shows the optimal fiber angles and the associated optimal fundamental frequencies ω_{opt} with respect to the L/r_1 ratio for $[\pm \theta/90_2/0]_{2s}$ laminated truncated conical shells with various end conditions and with N/N_{cr} equal to 0.2. From Fig. 4a we can see that the optimal fiber angle θ_{opt} of the laminated truncated conical shell seems to be insensitive to the boundary conditions. In addition, the optimal fiber angle θ_{opt} decreases with the increase of L/r_1 ratio. From Fig. 4b, we can observe that the optimal fundamental frequency ω_{opt} also decreases with the increase of L/r_1 ratio. The optimal fundamental frequency ω_{opt} is more sensitive to the

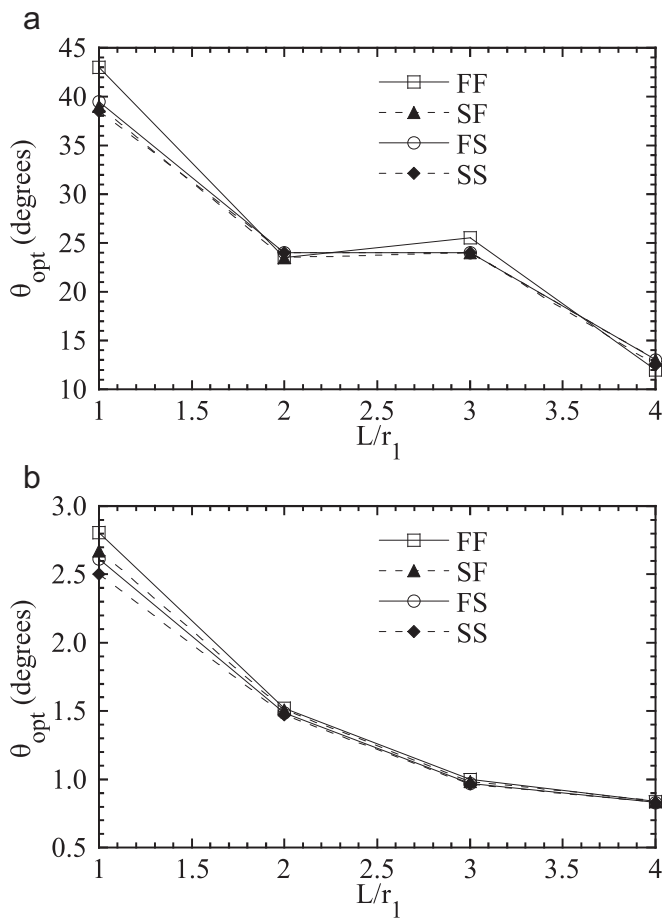


Fig. 13. Effect of end condition and L/r_1 ratio on optimal fiber angle and optimal fundamental frequency of $[\pm \theta/90_2/0]_{2s}$ laminated truncated conical shells with axial compressive force ($r_1 = 10$ cm, $r_2 = 8$ cm, $N/N_{cr} = 0.6$).

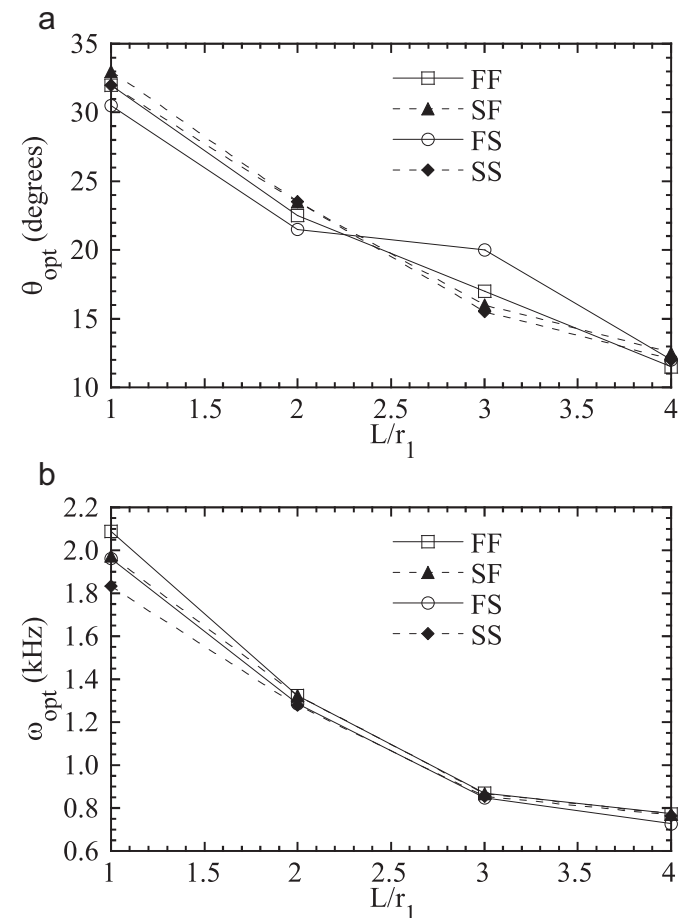


Fig. 14. Effect of end condition and L/r_1 ratio on optimal fiber angle and optimal fundamental frequency of $[\pm \theta/90_2/0]_{2s}$ laminated truncated conical shells with axial compressive force ($r_1 = 10$ cm, $r_2 = 8$ cm, $N/N_{cr} = 0.8$).

end conditions for short conical shell (say $L/r_1 = 1$) and is insensitive to the end conditions for long conical shell (say $L/r_1 = 4$). Nevertheless, among these shells under the same geometric configuration, the FF shells have the highest optimal fundamental frequencies, and the SS shells have the lowest optimal

fundamental frequencies. Though, the optimal fundamental frequencies ω_{opt} for the SF shells are slightly higher than those of the FS shells, their differences are hard to distinguish.

Figs. 5, 6 and 7 show the optimal fiber angle θ_{opt} and the associated optimal fundamental frequency ω_{opt} with respect to the

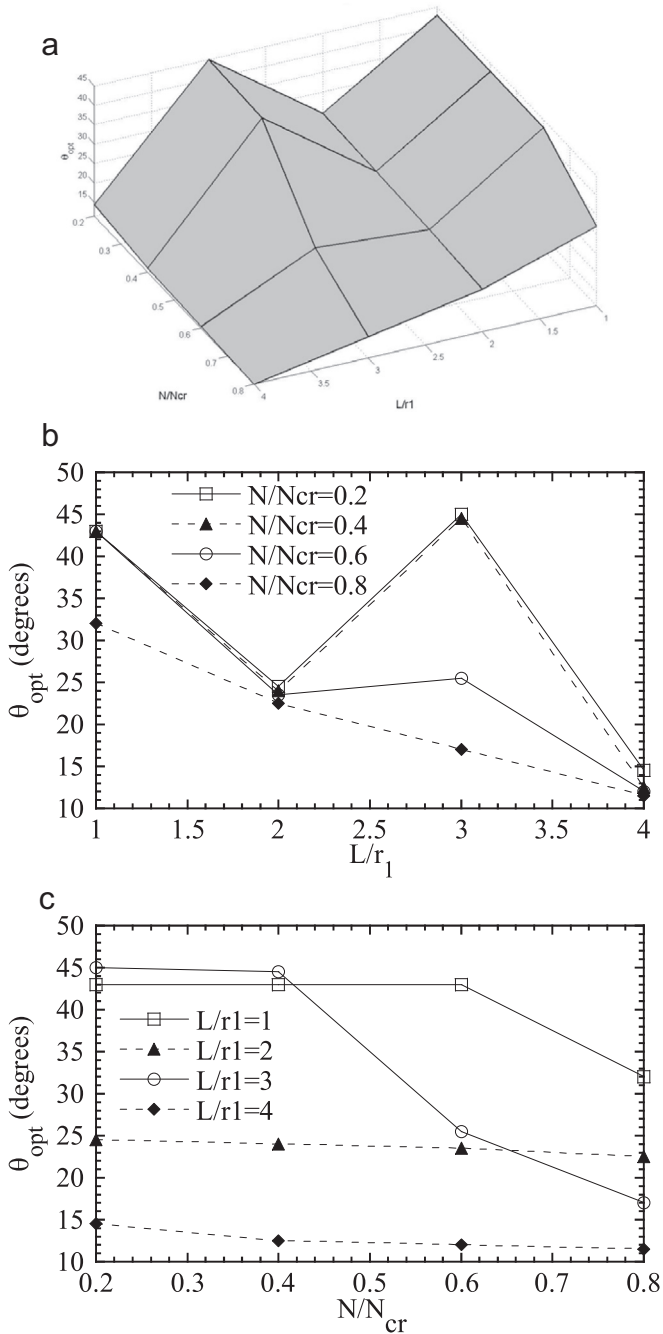


Fig. 15. Effect of L/r_1 ratio and N/N_{cr} ratio on optimal fiber angle of $[\pm \theta/90_2/0]_{2s}$ laminated truncated conical shells with two fixed ends ($r_1 = 10$ cm, $r_2 = 8$ cm).

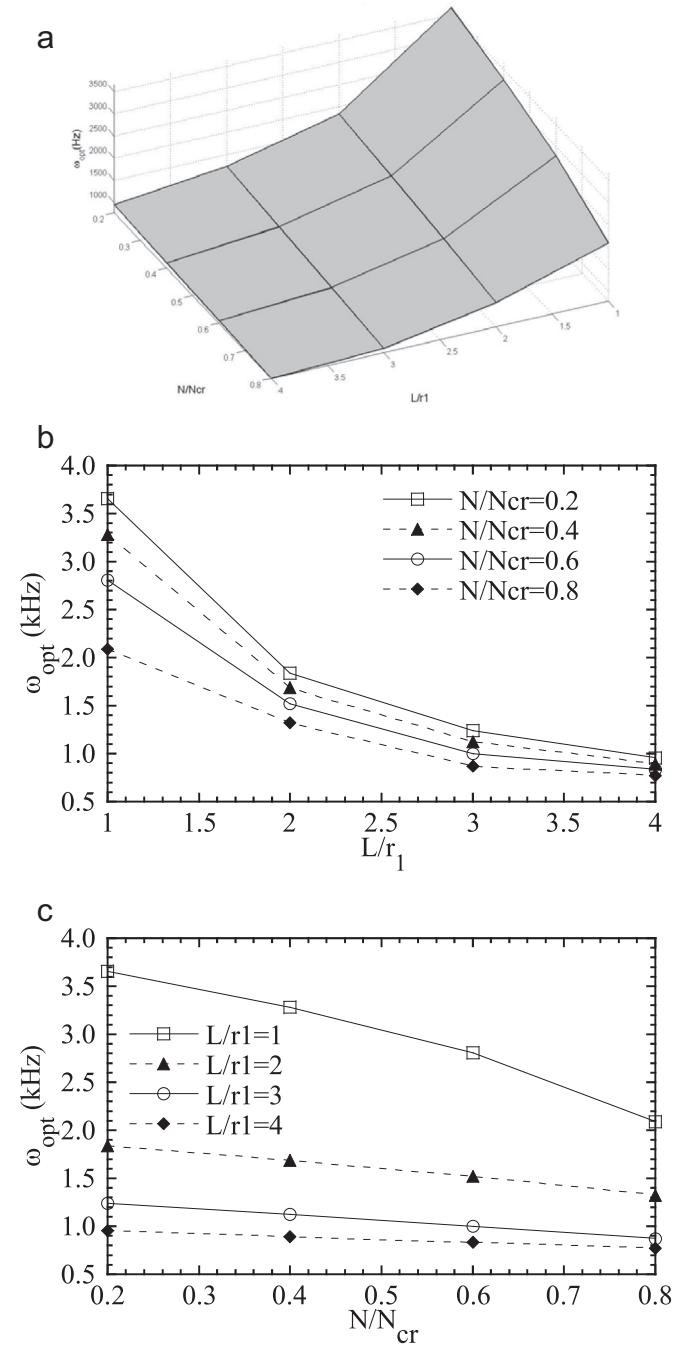


Fig. 16. Effect of L/r_1 ratio and N/N_{cr} ratio on optimal fundamental frequency of $[\pm \theta/90_2/0]_{2s}$ laminated truncated conical shells with two fixed ends ($r_1 = 10$ cm, $r_2 = 8$ cm).

L/r_1 ratio for $[\pm \theta/90_2/0]_{2s}$ laminated truncated conical shells with various end conditions and with N/N_{cr} equal to 0.4, 0.6 and 0.8. Generally, Figs. 5, 6 and 7 show similar trend as Fig. 4. The exceptions are the optimal fiber angles of conical shells with $L/r_1 = 3$ might be greater than those with $L/r_1 = 2$.

Fig. 8 shows the influence of L/r_1 ratio and N/N_{cr} ratio on optimal fiber angle of $[\pm \theta/90_2/0]_{2s}$ laminated truncated conical shells with two fixed ends. It can be seen that the optimal fiber angle θ_{opt} decreases with the increase of L/r_1 ratio (Fig. 8b). The exceptions are when $N/N_{cr} = 0.6$ and 0.8, the optimal fiber angles for conical shells with $L/r_1 = 3$ might be greater than those with $L/r_1 = 2$. In addition, the optimal fiber angle θ_{opt} decreases with the increase of the compressive force N (Fig. 8c). The exceptions are when $L/r_1 = 1$, the optimal fiber angles for conical shells increase slightly with the increase of N/N_{cr} ratio.

Fig. 9 shows the influence of L/r_1 ratio and N/N_{cr} ratio on optimal fundamental frequency of $[\pm \theta/90_2/0]_{2s}$ laminated truncated conical shells with two fixed ends. It can be clearly seen that the optimal fundamental frequency ω_{opt} decreases with the increase of L/r_1 ratio (Fig. 9b). In addition, the optimal fundamental frequency ω_{opt} decreases with the increase of the compressive force N (Fig. 9c) and the decrease in the optimal fundamental frequency for short conical shell (say $L/r_1 = 1$) is more significant than that for long conical shell (say $L/r_1 = 4$). Similar trends are also obtained for laminated truncated conical shells with other boundary conditions [34].

Fig. 10 shows the fundamental vibration modes of laminated truncated conical shells under optimal fiber angle θ_{opt} for $L/r_1 = 1$ and 4. It can be observed that under the same N/N_{cr} ratio and optimal fiber angle condition, the fundamental vibration mode of

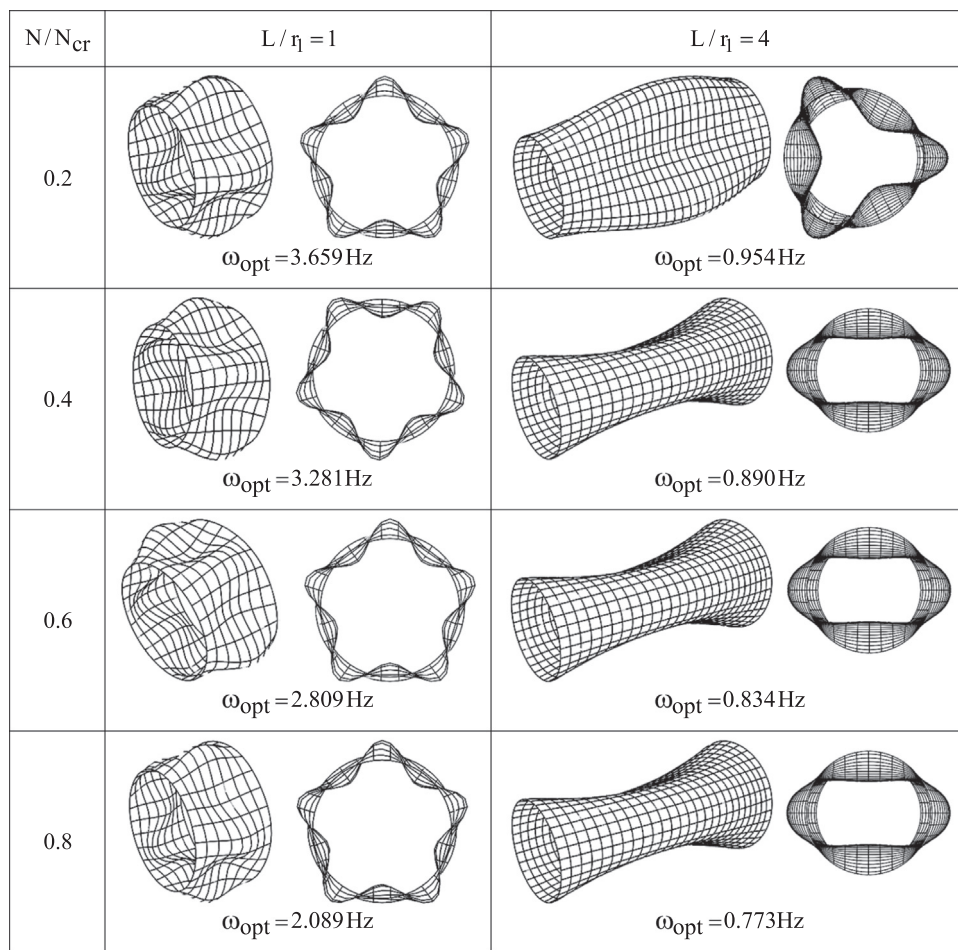


Fig. 17. Fundamental vibration modes of $[\pm \theta/90_2/0]_{2s}$ laminated truncated conical shells with two fixed ends and under optimal fiber angles ($r_1 = 10 \text{ cm}$, $r_2 = 8 \text{ cm}$).

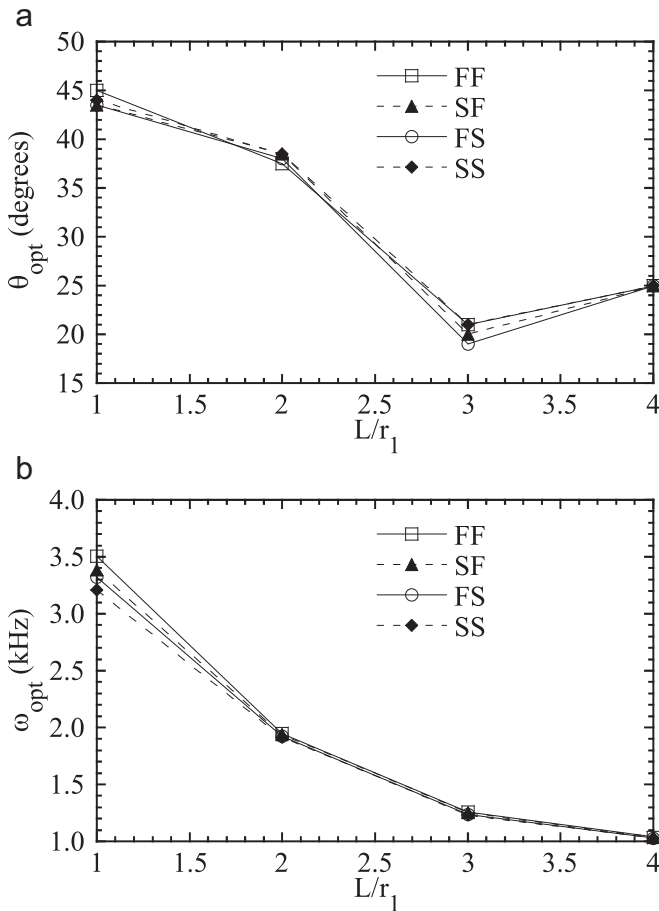


Fig. 18. Effect of end condition and L/r_1 ratio on optimal fiber angle and optimal fundamental frequency of $[\pm \theta/90_2/0]_{2s}$ laminated truncated conical shells with axial compressive force ($r_1 = 10$ cm, $r_2 = 6$ cm, $N/N_{cr} = 0.2$).

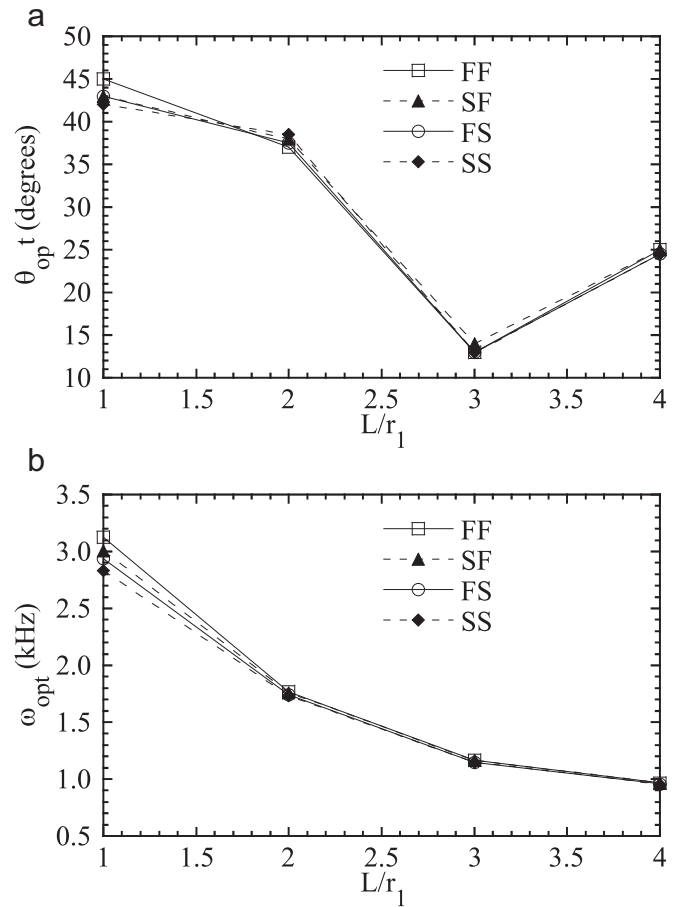


Fig. 19. Effect of end condition and L/r_1 ratio on optimal fiber angle and optimal fundamental frequency of $[\pm \theta/90_2/0]_{2s}$ laminated truncated conical shells with axial compressive force ($r_1 = 10$ cm, $r_2 = 6$ cm, $N/N_{cr} = 0.4$).

short conical shell has more wave numbers in the circumferential direction than that of long conical shell. Similar trends are also obtained for laminated truncated conical shells with other boundary conditions [34].

5.2. Laminated truncated conical shells with shell radius ratio $r_2/r_1 = 0.8$ and with various boundary conditions, lengths and axial compressive forces

In this section, laminated truncated conical shells subjected to axial compressive force and similar to those in previous section are analyzed except that the shell radius ratio r_2/r_1 is changed to 0.8. Fig. 11 shows the optimal fiber angle θ_{opt} and the associated optimal fundamental frequency ω_{opt} with respect to the L/r_1 ratio for $[\pm \theta/90_2/0]_{2s}$ laminated truncated conical shells with various end conditions and with N/N_{cr} equal to 0.2. From Fig. 11a, we can again see that the optimal fiber angles θ_{opt} of the laminated truncated conical shells seem to be insensitive to the boundary conditions. In addition, the optimal fiber angles θ_{opt} seem to be third-order polynomials of L/r_1 ratio. From Fig. 11b, we can again observe that the optimal fundamental frequency ω_{opt} decreases with the increase of L/r_1 ratio. The optimal fundamental frequency ω_{opt} is

sensitive to the end conditions when L/r_1 ratio is small and is insensitive to the end conditions when L/r_1 ratio is large. Again, among these shells under the same geometric configuration, the FF shells have the highest optimal fundamental frequencies, and the SS shells have the lowest optimal fundamental frequencies. Though, the optimal fundamental frequencies ω_{opt} for the SF shells are slightly higher than those of the FS shells, their differences are very small.

Figs. 12, 13 and 14 show the optimal fiber angle θ_{opt} and the associated optimal fundamental frequency ω_{opt} with respect to the L/r_1 ratio for $[\pm \theta/90_2/0]_{2s}$ laminated truncated conical shells with various end conditions and with N/N_{cr} equal to 0.4, 0.6 and 0.8. Generally, Figs. 12, 13 and 14 show similar trend as Fig. 11. However, as N/N_{cr} increase from 0.2 to 0.8, the optimal fiber angles of conical shells seem to change from third-order polynomials of L/r_1 ratio to first-order polynomials of L/r_1 ratio.

Fig. 15 shows the influence of L/r_1 ratio and N/N_{cr} ratio on optimal fiber angle of $[\pm \theta/90_2/0]_{2s}$ laminated truncated conical shells with two fixed ends. It can be more clearly see that as N/N_{cr} increase from 0.2 to 0.8, the optimal fiber angles of conical shells seem to change from a third-order polynomial of L/r_1 ratio to a first-order polynomial of L/r_1 ratio (Fig. 15b). In addition, the optimal fiber angle θ_{opt} seems to be insensitive to the N/N_{cr} ratio

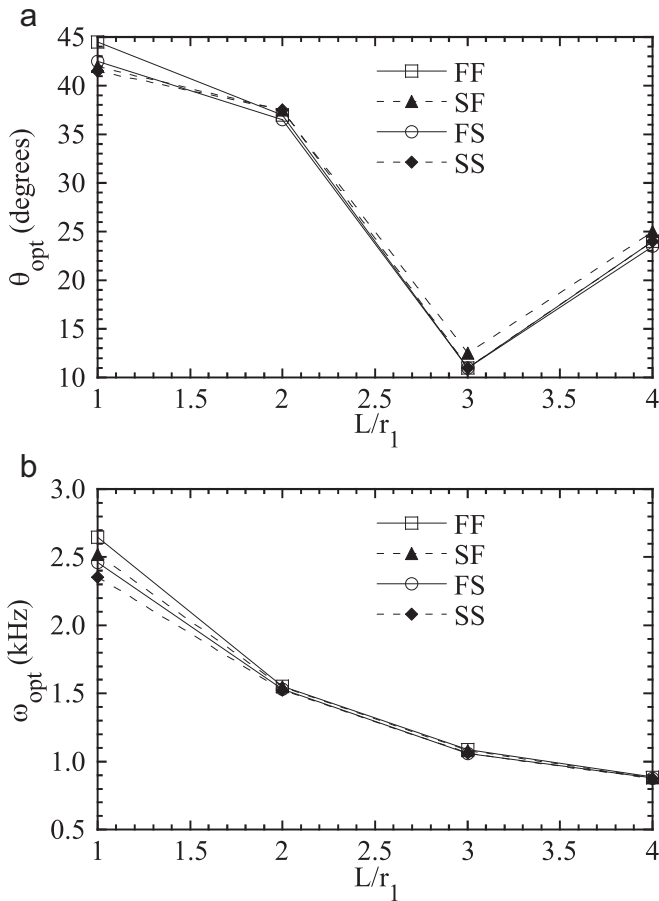


Fig. 20. Effect of end condition and L/r_1 ratio on optimal fiber angle and optimal fundamental frequency of $[\pm \theta/90_2/0]_{2s}$ laminated truncated conical shells with axial compressive force ($r_1 = 10$ cm, $r_2 = 6$ cm, $N/N_{cr} = 0.6$).

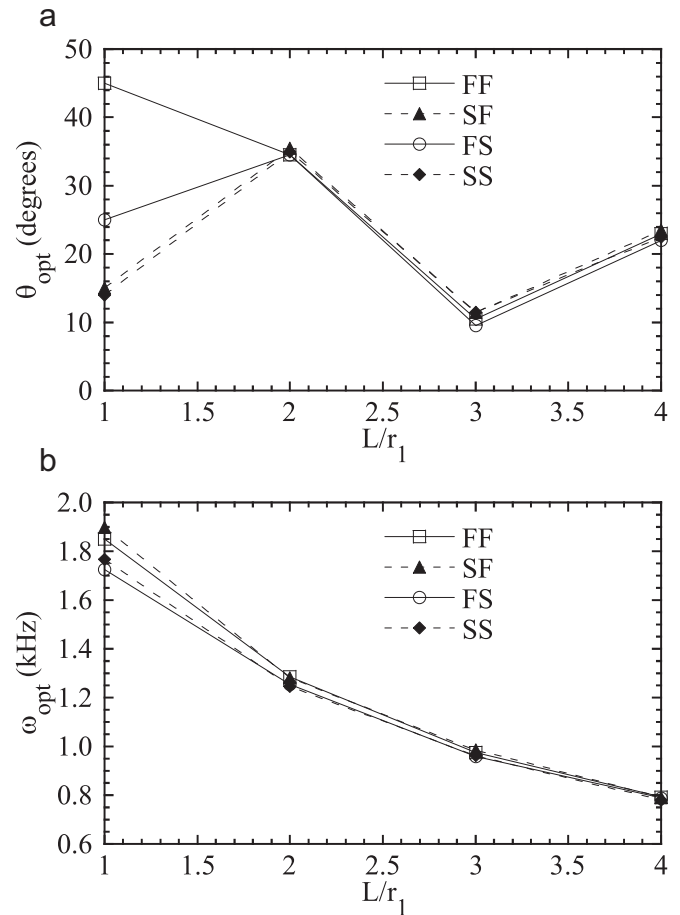


Fig. 21. Effect of end condition and L/r_1 ratio on optimal fiber angle and optimal fundamental frequency of $[\pm \theta/90_2/0]_{2s}$ laminated truncated conical shells with axial compressive force ($r_1 = 10$ cm, $r_2 = 6$ cm, $N/N_{cr} = 0.8$).

when $L/r_1 = 2$ and 4 (Fig. 15c).

Fig. 16 shows the influence of L/r_1 ratio and N/N_{cr} ratio on optimal fundamental frequency of $[\pm \theta/90_2/0]_{2s}$ laminated truncated conical shells with two fixed ends. It can be seen that the optimal fundamental frequency ω_{opt} decreases with the increase of L/r_1 ratio (Fig. 16b). In addition, the optimal fundamental frequency ω_{opt} decreases with the increase of the compressive force N (Fig. 16c) and the decrease in the optimal fundamental frequency for short conical shell is more significant than that for long conical shell. Similar trends are also obtained for laminated truncated conical shells with other boundary conditions [34].

Fig. 17 shows the fundamental vibration modes of laminated truncated conical shells under optimal fiber angle θ_{opt} for $L/r_1 = 1$ and 4. It can be observed that under the same N/N_{cr} ratio and optimal fiber angle condition, the fundamental vibration mode of short conical shell has more wave numbers in the circumferential direction than that of long conical shell. Similar trends are also obtained for laminated truncated conical shells with other boundary conditions [34].

5.3. Laminated truncated conical shells with shell radius ratio $r_2/r_1 = 0.6$ and with various boundary conditions, lengths and axial compressive forces

In this section, laminated truncated conical shells subjected to axial compressive force and similar to those in previous sections are analyzed except that the shell radius ratio r_2/r_1 is changed to 0.6. Fig. 18 shows the optimal fiber angle θ_{opt} and the associated optimal fundamental frequency ω_{opt} with respect to the L/r_1 ratio for $[\pm \theta/90_2/0]_{2s}$ laminated truncated conical shells with various end conditions and with N/N_{cr} equal to 0.2. From Fig. 18a, we can see that the optimal fiber angles θ_{opt} of the laminated truncated conical shells seem to be insensitive to the boundary conditions. In addition, the optimal fiber angles θ_{opt} seem to be third-order polynomials of L/r_1 ratio. From Fig. 18b, we can observe that the optimal fundamental frequency ω_{opt} decreases with the increase of L/r_1 ratio. The optimal fundamental frequency ω_{opt} is more sensitive to the end conditions when L/r_1 is small and is insensitive to the end conditions when L/r_1 ratio is large. Again, among these shells under the same geometric configuration, the FF shells have

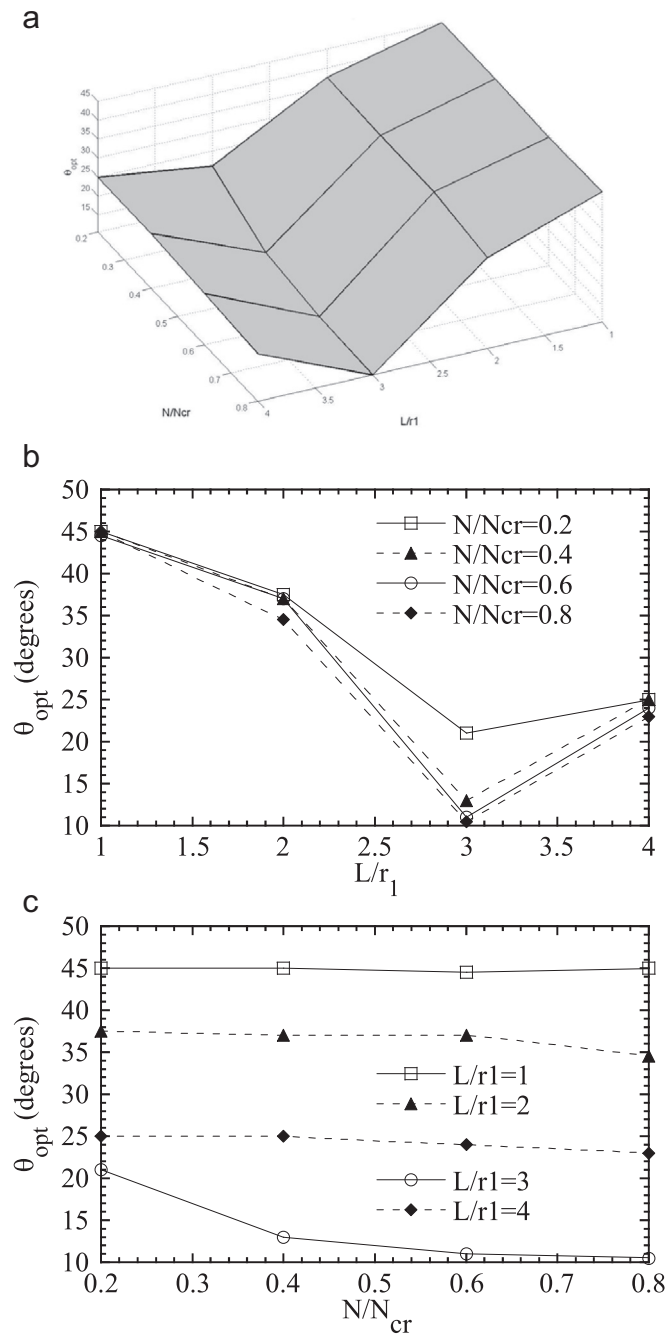


Fig. 22. Effect of L/r_1 ratio and N/N_{cr} ratio on optimal fiber angle of $[\pm \theta/90_2/0]_{2s}$ laminated truncated conical shells with two fixed ends ($r_1 = 10$ cm, $r_2 = 6$ cm).

the highest optimal fundamental frequencies, and the SS shells have the lowest optimal fundamental frequencies. Though, the optimal fundamental frequencies ω_{opt} for the SF shells are slightly higher than those of the FS shells, their differences are very small.

Figs. 19, 20 and 21 show the optimal fiber angle θ_{opt} and the associated optimal fundamental frequency ω_{opt} with respect to the L/r_1 ratio for $[\pm \theta/90_2/0]_{2s}$ laminated truncated conical shells with various end conditions and with N/N_{cr} equal to 0.4, 0.6 and 0.8. Generally, Figs. 19, 20 and 21 show similar trend as Fig. 18.

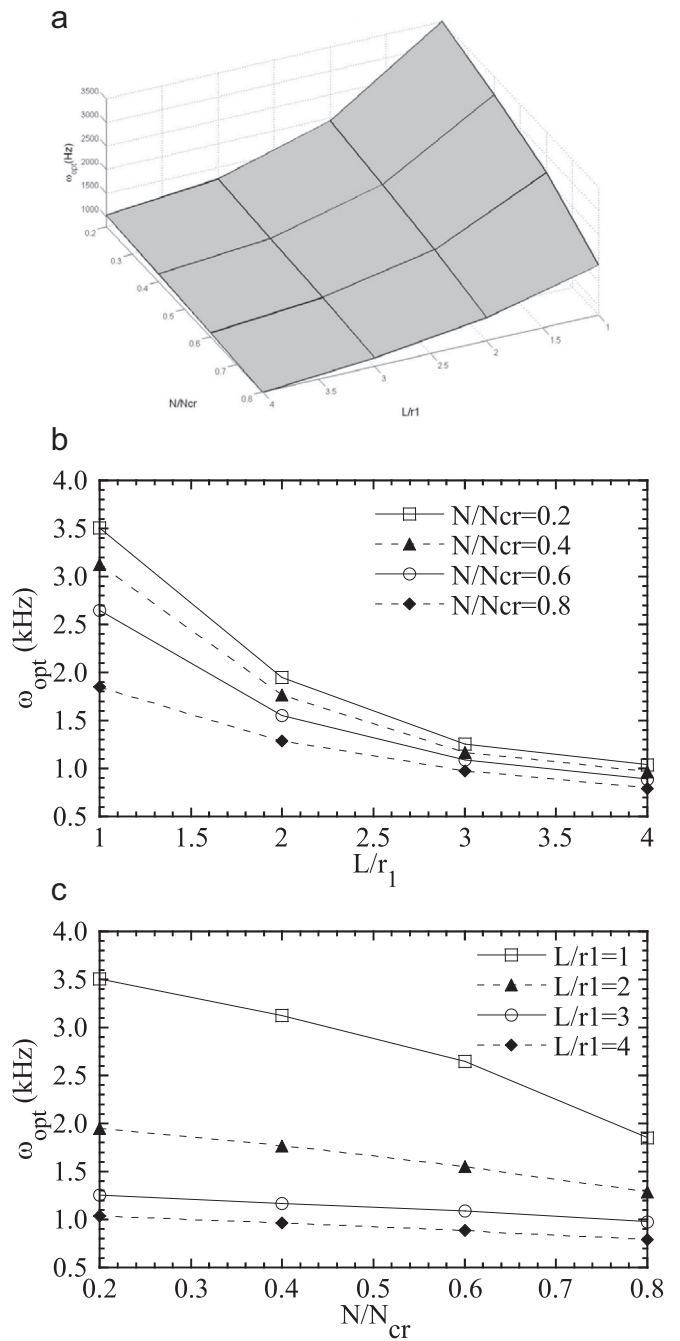


Fig. 23. Effect of L/r_1 ratio and N/N_{cr} ratio on optimal fundamental frequency of $[\pm \theta/90_2/0]_{2s}$ laminated truncated conical shells with two fixed ends ($r_1 = 10$ cm, $r_2 = 6$ cm).

Fig. 22 shows the influence of L/r_1 ratio and N/N_{cr} ratio on optimal fiber angle of $[\pm \theta/90_2/0]_{2s}$ laminated truncated conical shells with two fixed ends. It can be clearly see that the optimal fiber angles θ_{opt} of conical shells seem to be third-order polynomials of L/r_1 ratio (Fig. 22b). In addition, the optimal fiber angle θ_{opt} of conical shells with fixed L/r_1 ratio seems to be less sensitive to the N/N_{cr} ratio when N/N_{cr} ratio is large, say $N/N_{cr} > 0.4$ (Fig. 22c).

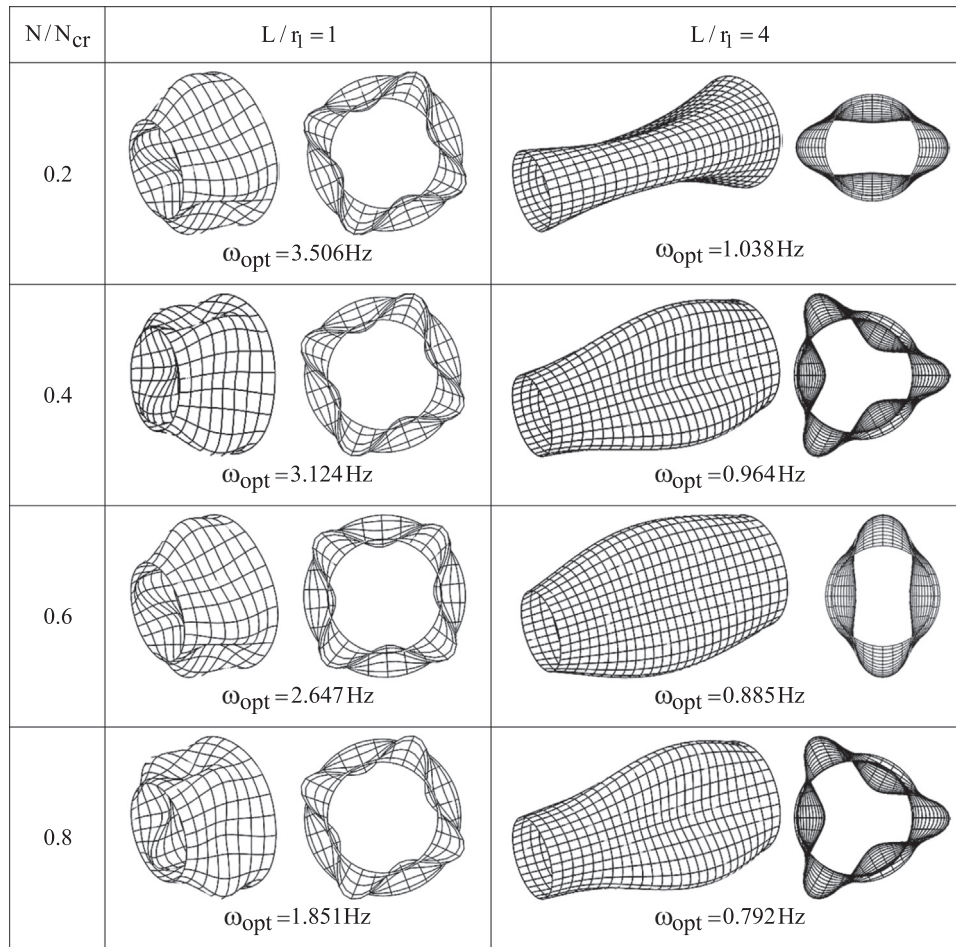


Fig. 24. Fundamental vibration modes of $[\pm \theta/90_2/0]_{2s}$ laminated truncated conical shells with two fixed ends and under optimal fiber angles ($r_1 = 10$ cm, $r_2 = 6$ cm).

Fig. 23 shows the influence of L/r_1 ratio and N/N_{cr} ratio on optimal fundamental frequency of $[\pm \theta/90_2/0]_{2s}$ laminated truncated conical shells with two fixed ends. It can be seen that the optimal fundamental frequency ω_{opt} decreases with the increase of L/r_1 ratio (Fig. 23b). In addition, the optimal fundamental frequency ω_{opt} decreases with the increase of the compressive force N (Fig. 23c) and the decrease in the optimal fundamental frequency for short conical shell is more significant than that for long conical shell. Similar trends are also obtained for laminated truncated conical shells with other boundary conditions [34].

Fig. 24 shows the fundamental vibration modes of laminated truncated conical shells under optimal fiber angle θ_{opt} for $L/r_1 = 1$ and 4. It can be observed that, under the same N/N_{cr} ratio and optimal fiber angle condition, the fundamental vibration mode of short conical shell has more wave numbers in the circumferential direction than that of long conical shell. Similar trends are also obtained for laminated truncated conical shells with other

boundary conditions [34]. Comparing Fig. 24 with Figs. 17 and 10, we can see that under the same L/r_1 ratio and optimal fiber angle condition, the fundamental vibration mode of the conical shell with small r_2/r_1 ratio has less wave numbers in the circumferential direction than the same conical shell with large r_2/r_1 ratio.

Figs. 25 and 26 show the influence of r_2/r_1 ratio and N/N_{cr} ratio on optimal fiber angle and optimal fundamental frequency of $[\pm \theta/90_2/0]_{2s}$ short laminated truncated conical shells with $L/r_1 = 1$ and with two fixed ends. From Fig. 25, we can see that the optimal fiber angles θ_{opt} of the conical shells seem to be insensitive to r_2/r_1 ratio when $N/N_{cr} \leq 0.6$. From Fig. 26, we can see that the optimal fundamental frequencies ω_{opt} of the conical shells increase with the increase of r_2/r_1 ratio and decrease with the increase of N/N_{cr} ratio.

Figs. 27 and 28 show the influence of r_2/r_1 ratio and N/N_{cr} ratio on optimal fiber angle and optimal fundamental frequency of $[\pm \theta/90_2/0]_{2s}$ long laminated truncated conical shells with $L/r_1 = 4$ and with two fixed ends. From Fig. 27, we can see that the optimal

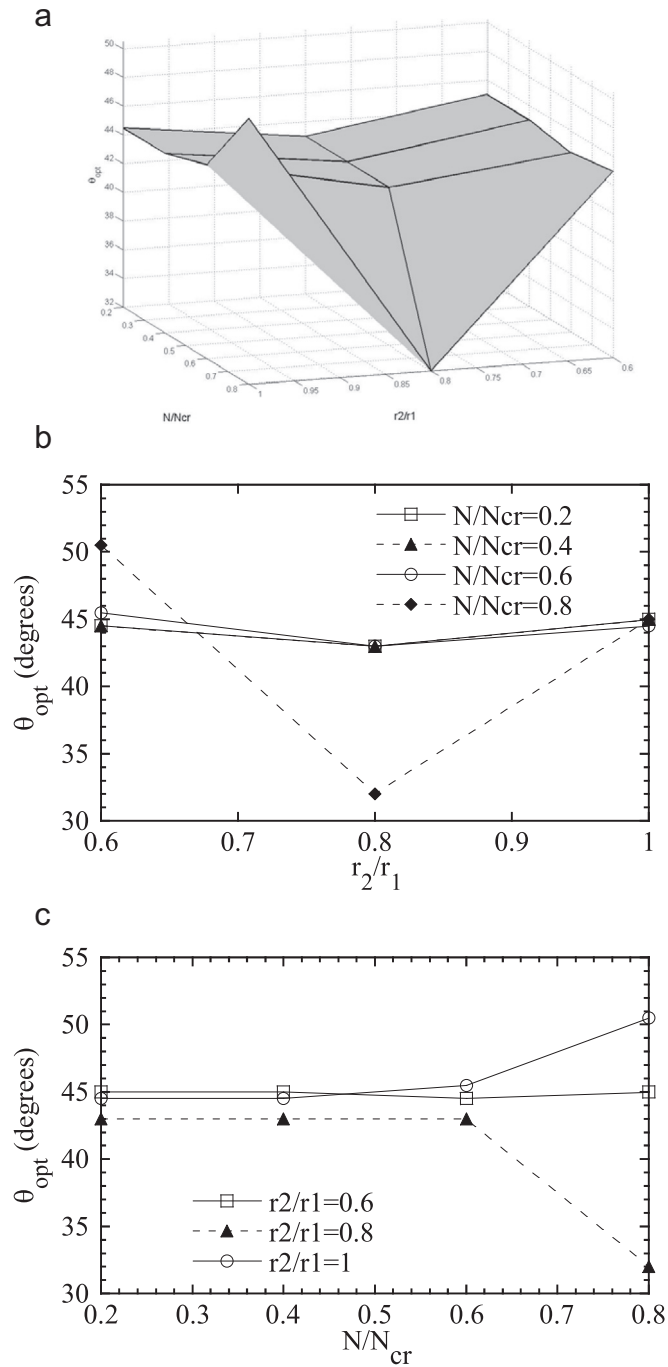


Fig. 25. Effect of r_2/r_1 ratio and N/N_{cr} ratio on optimal fiber angle of $[\pm \theta/90_2/0]_{2s}$ laminated truncated conical shells with two fixed ends ($r_1 = 10$ cm, $L/r_1 = 1$).

fiber angles θ_{opt} of the conical shells seem to be insensitive to N/N_{cr} ratio when $r_2/r_1 \leq 0.8$. From Fig. 28, we can see that the optimal fundamental frequencies ω_{opt} of the conical shells decrease with the increase of r_2/r_1 ratio and N/N_{cr} ratio.

6. Conclusions

Based on the numerical results of this investigation, the following conclusions could be drawn:

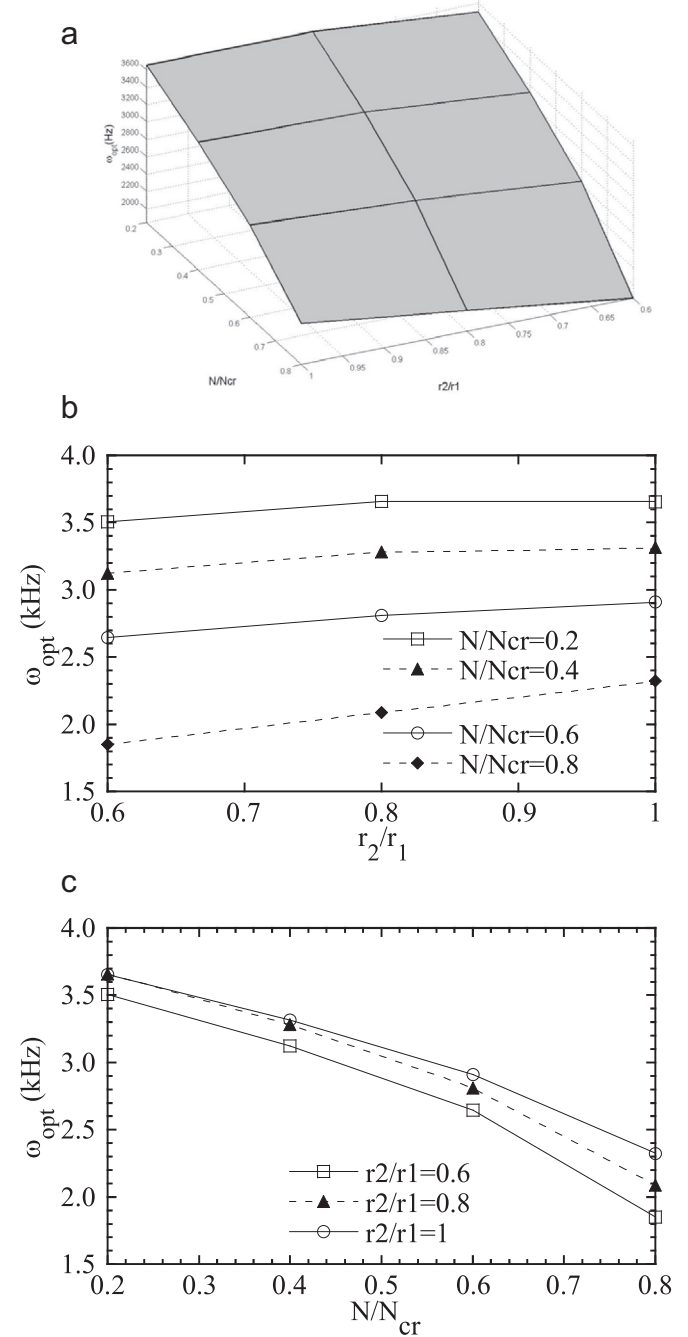


Fig. 26. Effect of r_2/r_1 ratio and N/N_{cr} ratio on optimal fundamental frequency of $[\pm \theta/90_2/0]_{2s}$ laminated truncated conical shells with two fixed ends ($r_1 = 10$ cm, $L/r_1 = 1$).

1. The optimal fiber angle θ_{opt} of the laminated truncated conical shell is insensitive to the boundary conditions.
2. The optimal fundamental frequency ω_{opt} of the laminated truncated conical shell decreases with the increase of L/r_1 ratio. The optimal fundamental frequency ω_{opt} is more sensitive to the end conditions when L/r_1 ratio is small and is insensitive to the end conditions when L/r_1 ratio is large.
3. The optimal fundamental frequency ω_{opt} of the laminated truncated conical shell decreases with the increase of N/N_{cr} ratio. This decrease in the optimal fundamental frequency for

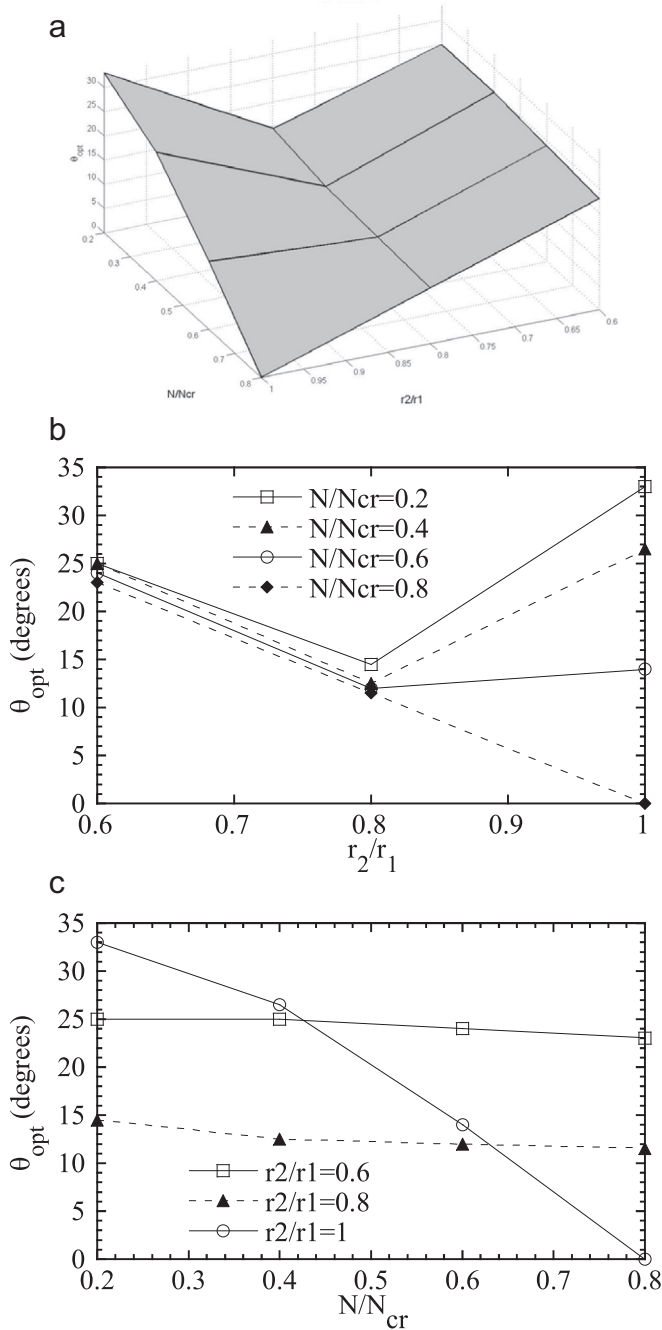


Fig. 27. Effect of r_2/r_1 ratio and N/N_{cr} ratio on optimal fiber angle of $[\pm \theta/90_2/0]_{2s}$ laminated truncated conical shells with two fixed ends ($r_1 = 10$ cm, $L/r_1 = 4$).

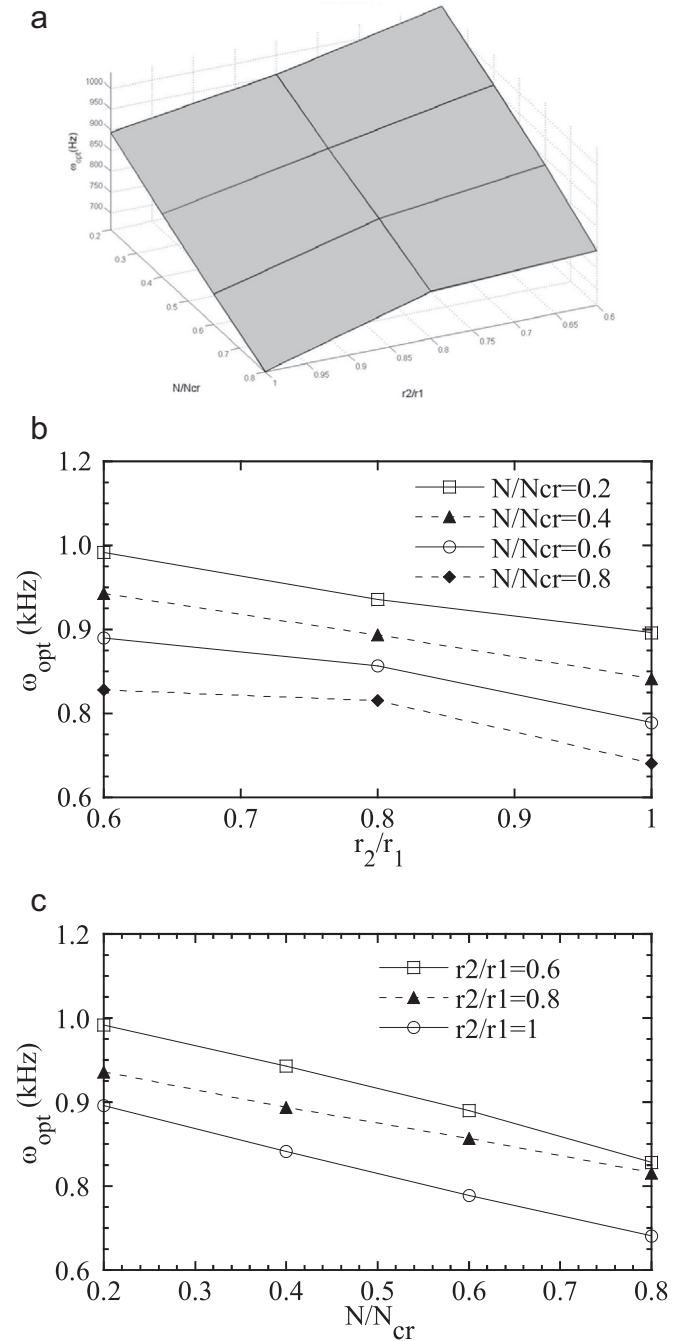


Fig. 28. Effect of r_2/r_1 ratio and N/N_{cr} ratio on optimal fundamental frequency of $[\pm \theta/90_2/0]_{2s}$ laminated truncated conical shells with two fixed ends ($r_1 = 10$ cm, $L/r_1 = 4$).

short conical shell (say $L/r_1 = 1$) is more significant than that for long conical shell (say $L/r_1 = 4$)

- For short laminated truncated conical shell (say $L/r_1 = 1$), its optimal fundamental frequency ω_{opt} increases with the increase of r_2/r_1 ratio.
- For long laminated truncated conical shell (say $L/r_1 = 4$), its optimal fundamental frequency ω_{opt} decreases with the increase of r_2/r_1 ratio.
- Under the same N/N_{cr} ratio and optimal fiber angle condition, the fundamental vibration mode of short conical shell has more wave numbers in the circumferential direction than that of long conical shell.

- Under the same L/r_1 ratio and optimal fiber angle condition, the fundamental vibration mode of the conical shell with small r_2/r_1 ratio has less wave numbers in the circumferential direction than the same conical shell with large r_2/r_1 ratio.

References

[1] D.J. Wilkins, C.W. Bert, D.M. Egle, Free vibrations of orthotropic sandwich conical shells with various boundary conditions, *J. Sound Vib.* 13 (1970)

- 211–228.
- [2] I. Sheinman, S. Greif, Dynamic analysis of laminated shells of revolution, *J. Compos. Mater.* 18 (1984) 200–215.
 - [3] N. Sankaranarayanan, K. Chandrasekaran, G. Ramaiyan, Free vibrations of laminated conical shells of variable thickness, *J. Sound Vib.* 123 (1988) 357–371.
 - [4] A. Kayran, J.R. Vinson, Free vibration analysis of laminated composite truncated circular conical shells, *AIAA J.* 28 (1990) 1259–1269.
 - [5] L. Tong, Free vibration of laminated conical shells including transverse shear deformation, *Int. J. Solids Struct.* 31 (1994) 443–456.
 - [6] K.N. Khatri, Vibrations of arbitrarily laminated fiber reinforced composite material truncated conical shell, *J. Reinf. Plast. Compos.* 14 (1995) 923–948.
 - [7] C.W. Lim, K.M. Liew, S. Kitipornchai, Vibration of cantilevered laminated composite shallow conical shells, *Int. J. Solids Struct.* 35 (1998) 1695–1707.
 - [8] A. Korjakin, R. Rikards, A. Chate, H. Altenbach, Analysis of free damped vibrations of laminated composite conical shells, *Compos. Struct.* 41 (1998) 39–47.
 - [9] H.-T. Hu, S.-C. Ou, Maximization of the fundamental frequencies of laminated truncated conical shells with respect to fiber orientations, *Compos. Struct.* 52 (2001) 265–275.
 - [10] Ö. Civalek, Numerical analysis of free vibrations of laminated composite conical and cylindrical shells: Discrete singular convolution (DSC) approach, *J. Comput. Appl. Math.* 205 (2007) 251–271.
 - [11] S. Dey, A. Karmakar, Natural frequencies of delaminated composite rotating conical shells—a finite element approach, *Finite Elem. Anal. Des.* 56 (2012) 41–51.
 - [12] K. Daneshjou, M. Talebitooti, R. Talebitooti, Free vibration and critical speed of moderately thick rotating laminated composite conical shell using generalized differential quadrature method, *Appl. Math. Mech.* 34 (2013) 437–456.
 - [13] K.R. Sivasdas, Vibration analysis of pre-stressed thick circular conical composite shells, *J. Sound Vib.* 186 (1995) 87–97.
 - [14] C.-S. Chen, W.-S. Cheng, R.-D. Chien, J.-L. Doong, Large amplitude vibration of an initially stressed cross ply laminated plates, *Appl. Acoust.* 63 (2002) 939–956.
 - [15] A.K. Nayak, S.S.J. Moy, R.A. Sheno, A higher order finite element theory for buckling and vibration analysis of initially stressed composite sandwich plates, *J. Sound Vib.* 286 (2005) 763–780.
 - [16] A. Chakrabarti, P. Topdar, A.H. Sheikh, Vibration of pre-stressed laminated sandwich plates with interlaminar imperfections, *J. Vib. Acoust.* 128 (2006) 673–681.
 - [17] H.-T. Hu, W.-K. Tsai, Maximization of the fundamental frequencies of axially compressed laminated plates against fiber orientation, *AIAA J.* 27 (2009) 916–922.
 - [18] H.-T. Hu, J.-M. Chen, Maximization of fundamental frequencies of axially compressed laminated curved panels against fiber orientation CMC: Computers, Mater. Contin. 28 (2012) 181–211.
 - [19] H.-T. Hu, H.-W. Peng, Maximization of fundamental frequency of axially compressed laminated curved panels with cutouts, *Compos. B: Eng.* 47 (2013) 8–25.
 - [20] S. Abrate, Optimal design of laminated plates and shells, *Compos. Struct.* 29 (1994) 269–286.
 - [21] G. Teters, Multicriteria optimization of a composite cylindrical shell subjected to thermal and dynamics actions, *Mech. Compos. Mater.* 40 (2004) 489–494.
 - [22] U. Topal, Multiobjective optimization of laminated composite cylindrical shells for maximum frequency and buckling load, *Mater. Des.* 30 (2009) 2584–2594.
 - [23] Ö. Civalek, Vibration analysis of conical panels using the method of discrete singular convolution, *Commun. Numer. Methods Eng.* 24 (2008) 169–181.
 - [24] Ö. Civalek, Vibration analysis of laminated composite conical shells by the method of discrete singular convolution based on the shear deformation theory, *Compos. B: Eng.* 45 (2013) 1001–1009.
 - [25] C. Shu, Free vibration analysis of composite laminated conical shells by generalized differential quadrature, *J. Sound Vib.* 194 (1996) 587–604.
 - [26] K.M. Liew, T.Y. Ng, X. Zhao, Free vibration analysis of conical shells via the element-free kp-Ritz method, *J. Sound Vib.* 281 (2005) 627–645.
 - [27] L.A. Schmit, Structural synthesis—its genesis and development, *AIAA J.* 19 (1981) 1249–1263.
 - [28] G.N. Vanderplaats, *Numerical Optimization Techniques for Engineering Design with Applications*, McGraw-Hill, 1984.
 - [29] R.T. Haftka, Z. Gürdal, M.P. Kamat, *Elements of Structural Optimization*, Second Revised Edition, Kluwer Academic Publishers, 1990.
 - [30] Dassault Systèmes Corporation, *SIMULIA Abaqus Analysis User's Manuals, Theory Manuals and Example Problems Manuals*, 2014 (Version 6.14, France).
 - [31] J.M. Whitney, Shear correction factors for orthotropic laminates under static load, *J. Appl. Mech.* 40 (1973) 302–304.
 - [32] R.D. Cook, D.S. Malkus, M.E. Plesha, R.J. Witt, *Concepts and Applications of Finite Element Analysis*, Fourth Edition, John Wiley & Sons Inc., 2002.
 - [33] E.F. Crawley, The natural modes of graphite/epoxy cantilever plates and shells, *J. Compos. Mater.* 13 (1979) 195–205.
 - [34] P.-J. Chen, Maximization of Fundamental Frequencies of Axially Compressed Laminated Cones against Fiber Orientations (M.Sc. thesis), Department of Civil Engineering, National Cheng Kung University, Tainan, Taiwan, 2011.